Laser excitation studies and crystal-field analysis of ZnO:Tb^{3+} and ZnO:Eu^{3+} powders

N A Bhebhe[1], M Mujaji[1], D Wamwangi[1], L F Koao[2] and F B Dejene[2]

[1] School of Physics and DST-NRF Centre of Excellence in Strong Materials, University of the Witwatersrand, Johannesburg, Wits 2050, South Africa
[2] Department of Physics, University of the Free State (Qwaqwa Campus), Private Bag X13, Phuthaditjhaba ZA 9866, South Africa

E-mail: Nkosiphile.Bhebhe@students.wits.ac.za

Abstract. Results from laser excitation studies of Tb^{3+} ions and Eu^{3+} ions in zinc oxide (ZnO) powders are presented; rare-earth doped ZnO (ZnO:RE^{3+}) is currently of great interest as a prospective solid-state laser matrix and for optoelectronic device applications. The chemical bath deposition technique was utilized for synthesizing the ZnO:Tb^{3+} and ZnO:Eu^{3+} powders. Photoluminescence spectra of the pellet samples were obtained in the 460 – 900 nm range. The spectra exhibit sharp emission lines superimposed on a broad emission background with 457.9 nm, 476.5 nm and 488.0 nm argon laser-line excitation. The sharp peaks are attributed to the $^5D_4 \rightarrow {}^7F_J$ (J = 0, 1, 2, 3, 4, 5, 6) and the $^5D_0 \rightarrow {}^7F_J$ (J = 0, 1, 2, 3, 4) electronic transitions of Tb^{3+} and Eu^{3+}, respectively. Crystal-field energy levels for the Tb^{3+} ion and the Eu^{3+} ion occupying a C_{3v} symmetry site were deduced.

1. Introduction

Semiconductors such as zinc oxide (ZnO) and gallium nitride (GaN) are of great importance to the optoelectronic industry because of their inherent optical and electronic properties [1,2]. ZnO has drawn considerable interest because of its superior properties which include a wide band gap (3.36 eV) [3] and a large exciton binding energy of 60 meV [1]. Furthermore, ZnO is a cheap, chemically and thermally stable material [4].

Optical studies have shown ZnO to exhibit a broad emission in the visible region of the electromagnetic spectrum [1,4,5]. The broad emission has been attributed to deep level transitions within the band gap due to intrinsic ZnO defects such as zinc vacancies and oxygen vacancies [3,4]. To improve on the visible emission, studies on rare earth (RE^{3+}) doped ZnO continue to be pursued with successful incorporation of RE^{3+} ions such as trivalent terbium (Tb^{3+}) [1,6] and trivalent europium (Eu^{3+}) [7]. In the literature, it is suggested that the RE^{3+} ion resides at either a Zn^{2+} lattice site or an interstitial position [6,7,8] with a neighboring zinc vacancy for charge compensation [6]. However, there has been no experimental verification of the RE^{3+} location. Intense green and red emission bands have been observed for ZnO:Tb^{3+} [1,6] and ZnO:Eu^{3+} [7], respectively, with ultra-violet excitation. RE^{3+} doping therefore significantly enhances visible luminescence in ZnO and could be useful for solid-state laser development and for optoelectronic device applications. The relatively intense peaks are attributed to the RE^{3+} intra-4f radiative transitions [1,7]. The narrow line widths are

a result of the free ion like behaviour of the RE^{3+} ion due to 5s and 5p shielding of the 4f orbital from the ligand environment [1].

Among the many different techniques of synthesizing RE^{3+} doped semiconductors [3,5] interest has shifted towards semiconductor powders [1,7]. Powder synthesis provides a simple and low-cost procedure for the incorporation of RE^{3+} dopants into semiconductors [2]. In particular, the chemical bath deposition method is a low temperature (80 °C) technique.

In the literature, studies of ZnO:Tb^{3+} and ZnO:Eu^{3+} have focused on ultra-violet excitation and visible emission for white light production [1,7]. In this work, visible-region excitation and visible-region emission studies of ZnO:Tb^{3+} and ZnO:Eu^{3+} are presented. Crystal-field analyses of Tb^{3+} ions and Eu^{3+} ions occupying a C_{3v} symmetry site have been performed and crystal-field energy levels deduced. This study of the visible-region emission characteristics of Tb^{3+} ions and Eu^{3+} ions in ZnO is important for development of solid-state lasers and for other optoelectronic device applications. Furthermore, the effect of the incorporation of RE^{3+} ions in the ZnO structure has been investigated.

2. Experimental aspects

The chemical bath deposition method was utilized to synthesize Tb^{3+} and Eu^{3+} doped as well as undoped ZnO powders. The precursors were analytical grade 0.03 mol of zinc acetate ($Zn(CH_3COO)_2 \cdot 2H_2O$) dissolved in 60 ml of deionised water, 0.09 mol of thiourea ($(NH_2)_2CS$) dissolved in 500 ml of deionised water, 123.5 ml of ammonia (25% NH_3) dissolved in 500 ml of deionised water; these were mixed in volume ratios of 60 ml : 60 ml : 60 ml. To obtain a 1.0 mol% RE^{3+} dopant concentration 0.0003 mol of either terbium nitrate ($Tb(NO_3)_3 \cdot 6H_2O$) or of europium acetate ($Eu(CH_3COO)_3 \cdot 2H_2O$), both of 99.9 % purity, were added. The detailed preparation procedure was as presented by Koao et al. [7] and the resulting powder was pressed using a hydraulic press at 80 kN to obtain a pellet of diameter 8 mm and a thickness of 2 mm. The pellets were annealed at 700 °C for two hours in air.

Room temperature photoluminescence measurements were carried out on the pellets, using 457.9 nm (21 838.8 cm^{-1}), 476.5 nm (20 986.4 cm^{-1}) and 488.0 nm (20 491.8 cm^{-1}) excitation lines of the Spectra Physics 2080 argon ion laser. The emission was detected using a Burle C31034-A02 photomultiplier tube coupled to a McPherson 2062DP monochromator together with an SRS preamplifier and photon counter. Typically, laser powers of 35 mW and monochromator slit-widths of 250 μm were used. Spectra were recorded in the 460 – 900 nm range. The 515 nm and 495 nm long pass filters were used with the 488.0 nm and the 476.5 nm laser lines, respectively. Grazing incidence x-ray diffraction (GIXRD) measurements were also carried out on all the samples using the 0.154 nm Cu K_α wavelength of the Bruker D8 Discover at $\omega = 1°$. The measurements were carried out in the range $20° \leq 2\theta \leq 80°$.

3. Results and discussion

3.1. XRD studies

The grazing incidence XRD patterns obtained at room temperature for pristine ZnO, 1.0 mol% Tb^{3+} doped and 1.0 mol% Eu^{3+} doped ZnO powders are presented in figure 1 for the as-prepared and the annealed samples. The annealing treatment was carried out so as to remove precursor impurity phases that were observed in the as-prepared samples. GIXRD results show the presence of a wurtzite ZnO phase ((100), (002), (101), (102), (110), (103), (112) and (202)) in all the annealed samples; there are no phase changes arising from the addition of the Eu^{3+} ions and the Tb^{3+} ions. This supports the suggestion that the incorporation of the Tb^{3+} ions and Eu^{3+} ions into the host matrix is substitutional in nature [6,7,8]. In this study, it was not possible to experimentally identify the lattice location of the RE^{3+} ions. However in the literature, the Tb^{3+} ion (0.92 Å) and the Eu^{3+} ion (0.95 Å) have been proposed to occupy the Zn^{2+} (0.74 Å) lattice site in the ZnO structure [4,7].

The observed broadening of the XRD peaks has been attributed to the small crystallite sizes of the powders [9]. As such the average crystallite sizes of the samples were calculated from the Debye

Scherrer formula [4]. The lattice constants 'a' and 'c' are presented in table 1 together with the crystallite sizes 'D'.

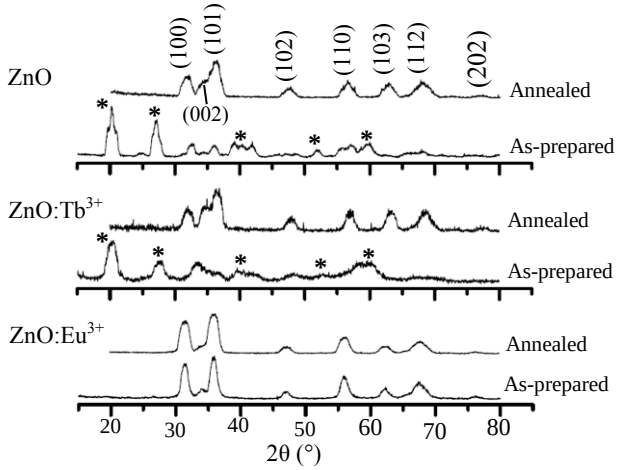

Figure 1. Room temperature grazing incidence XRD patterns for as-prepared and annealed pristine ZnO, 1.0 mol% Tb^{3+} doped and 1.0 mol% Eu^{3+} doped ZnO powders. (*) Zinc acetate precursor impurity.

The XRD patterns show a hexagonal wurtzite ZnO structure for all the samples. Therefore, the incorporation of the Tb^{3+} ions and the Eu^{3+} ions does not result in an effective change of the ZnO host structure.

Table 1. Lattice constants and crystallite sizes for undoped, Tb^{3+} and Eu^{3+} doped ZnO powders.

Sample	Lattice constants (±0.006 nm)		Crystallite size (±1 nm)
	a (nm)	c (nm)	D (nm)
ZnO	0.326	0.519	9
ZnO:Eu^{3+}	0.327	0.523	9
ZnO:Tb^{3+}	0.322	0.517	10

3.2. Laser excited photoluminescence

Photoluminescence spectra of undoped as well as 1.0 mol% Tb^{3+} and 1.0 mol% Eu^{3+} doped ZnO pellets were obtained at room temperature with argon laser excitation. The 457.9 nm, 476.5 nm and 488.0 nm excitation wavelengths were used. Although there are spectral variations in the doped samples arising from the different excitation lines, the same spectrum was obtained for the undoped sample with all three excitation lines. The 488.0 nm spectrum included in figures 2(a) and 3(a) was of slightly better intensity. The photoluminescence spectra of the annealed samples showed no significant changes in the Tb^{3+} ion and Eu^{3+} ion emissions compared to the un-annealed (as-prepared) samples. The spectra of the as-prepared samples are presented in figures 2(a) and 3(a).

The spectrum for undoped ZnO (figures 2 and 3) shows a broad emission band with almost uniform intensity from 550 nm to about 700 nm, followed by a gradual decrease in intensity with increase in wavelength thereafter. This emission is attributed to deep level transitions within the ZnO band gap due to intrinsic defects [3,4].

For ZnO:1.0 mol% Tb^{3+}, electronic transitions from the $^5D_4$ multiplet to all the ^7F_J (J = 0, 1, 2, 3, 4, 5, 6) multiplets were observed (figure 2(a)). Energy transfer from the intrinsic defects in the host lattice to the RE^{3+} ion results in the population of the Tb^{3+} $^5D_4$ multiplet [1,4]. Transitions to the $^7F_2$, $^7F_1$ and $^7F_0$ multiplets were quite weak by comparison (figure 2(a) inset). With either 457.9 nm or 476.5 nm excitation the sample exhibits a broad emission band spanning the visible region of the electromagnetic spectrum on which relatively intense peaks are superimposed. As the excitation wavelength is increased from 457.9 nm to 488.0 nm the broad emission band is increasingly suppressed while the Tb^{3+} emission bands increase in intensity. The $^5D_4 \rightarrow {}^7F_{6,5,4,3}$ emission bands are

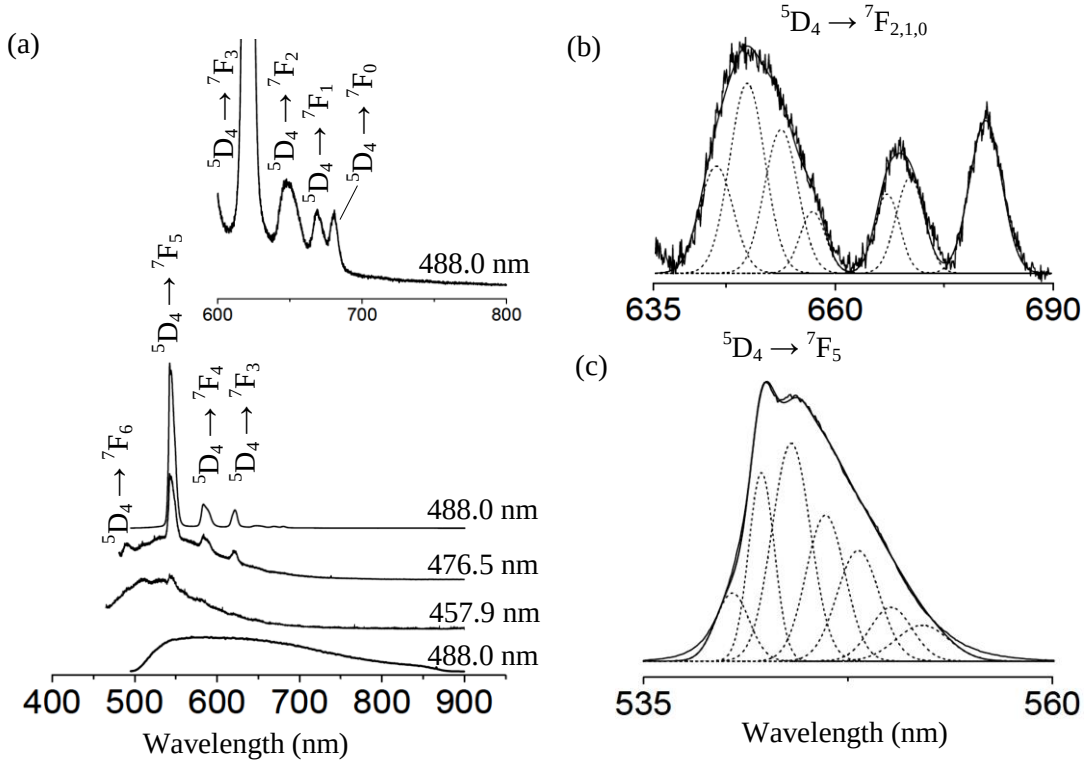

Figure 2. (a) Room temperature photoluminescence spectra of ZnO:Tb^{3+} and undoped ZnO pellets. (b) and (c) Gaussian peak fitted emission bands. The excitation wavelengths are as indicated while the peak labels identify the multiplets associated with each transition band.

as reported in the literature from ultra-violet excitation [1,4] while the $^5D_4 \rightarrow {}^7F_{2,1,0}$ emission bands have not been reported before. The 488.0 nm excitation wavelength is in resonance with the $^5D_4$ multiplet and as a result, the emission is significantly stronger rendering the weaker transitions observable.

Knowledge of the RE^{3+} ion site symmetry in the host matrix is important for determining the RE^{3+} ion energy levels resulting from crystal-field effects [10]. It is from the site symmetry and the selection rules that RE^{3+} ion transitions can be assigned to specific originating and terminating crystal-field energy levels, thereby determining the energy level scheme of the RE^{3+} ion in a particular host lattice [10]. Pereira et al. [8] proposed a C_{3v} site symmetry for the RE^{3+} ion at a Zn^{2+} lattice site and this configuration is adopted for the analyses presented here. In this work, the number of crystal-field energy levels expected for a C_{3v}-symmetry site were determined from group theory decomposition tables [11]. However, electronic transitions between some of the crystal-field energy levels are forbidden resulting in fewer experimentally-determined levels for some of the multiplets.

In order to deduce the crystal-field energy levels from the observed photoluminescence spectra, Gaussian peak profiles were fitted to the observed Tb^{3+} emission bands as demonstrated in figure 2(b) and (c). Governed by the selection rules, fittings were carried out starting with the $^7F_0$ multiplet as it has only one energy level and therefore a single transition. Each Gaussian peak in the emission band represented an electronic transition from a crystal-field energy level in the $^5D_4$ multiplet to a crystal-field energy level in each of the ^7F_J multiplets. From the results, two crystal-field energy levels of the excited $^5D_4$ multiplet were deduced to be at 20 483 cm^{-1} (488.2 nm) and 20 602 cm^{-1} (485.5 nm). At room temperature electrons have sufficient thermal energy to occupy the second level of the $^5D_4$ multiplet resulting in transitions from the higher level (20 602 cm^{-1}) being present as well and mixed in with those from the lower level at 20 483 cm^{-1}. The crystal-field energy levels determined here for the

$^5D_4$ and the ^7F_J (J = 0, 1, 2, 3, 4, 5, 6) multiplets of Tb^{3+} in ZnO are presented in table 2; the number in brackets is the total number of levels for each multiplet as obtained from the decomposition tables.

Table 2. Crystal-field energy levels of the Tb^{3+} ion in ZnO in cm^{-1} (± 2 cm^{-1}).

Multiplet	$^7F_6$ (9)	$^7F_5$ (7)	$^7F_4$ (6)	$^7F_3$ (5)	$^7F_2$ (3)	$^7F_1$ (2)	$^7F_0$ (1)	$^5D_4$ (6)
Levels	0	2 046	3 287	4 330	5 065	5 495	5 794	20 483
	95	2 106	3 340	4 359	5 162	5 571		20 602
	199	2 178	3 398	4 399	5 267			
	408	2 245	3 465	4 439				
		2 301	3 531	4 486				
		2 377	3 597					

For ZnO:1.0 mol% Eu^{3+}, electronic transitions from the $^5D_0$ multiplet to the ^7F_J (J = 0, 1, 2, 3, 4) multiplets were observed (figure 3(a)). In addition, transitions from the $^5D_1$ multiplet to the $^7F_3$ and $^7F_4$ multiplets overlapped with the $^5D_0 \rightarrow {}^7F_{1,2}$ transitions, respectively. All three excitation wavelengths show Eu^{3+} ion related emission bands also superimposed on a broad emission background. The emission spectrum obtained with 457.9 nm excitation was quite noisy and had the least intense Eu^{3+} emission bands in comparison to those for the 476.5 nm and 488.0 nm excitation lines hence it is not included in figure 3(a). These emission bands have been reported in the literature from ultra-violet excitation studies but with no further analysis [7]. Increasing the excitation wavelength from 457.9 nm to 488.0 nm resulted in a relative increase in the intensity of the Eu^{3+} emission bands.
The Eu^{3+} crystal-field energy levels were deduced using the same deconvolution procedure as for Tb^{3+}, as in figure 3(b) and (c). The position of the $^5D_1$ multiplet was deduced from the $^5D_1 \rightarrow {}^7F_{3,4}$ transitions although it was not possible to identify the $^5D_1 \rightarrow {}^7F_{0,1,2}$ transitions. From the results, the crystal-field energy level of the $^5D_0$ multiplet was deduced to be at 17 259 cm^{-1} (579.4 nm) while the lower-lying crystal-field energy level of the $^5D_1$ multiplet was placed at 18 847 cm^{-1} (530.6 nm). The crystal-field energy levels deduced for the $^5D_{0,1}$ and the ^7F_J (J = 0 to 4) multiplets of Eu^{3+} in ZnO are presented in table 3.

The photoluminescence spectra (figures 2 and 3) show strong green emission for ZnO:Tb^{3+} and strong red emission for ZnO:Eu^{3+}. In general, the Eu^{3+} ion emission was weaker than the Tb^{3+} ion

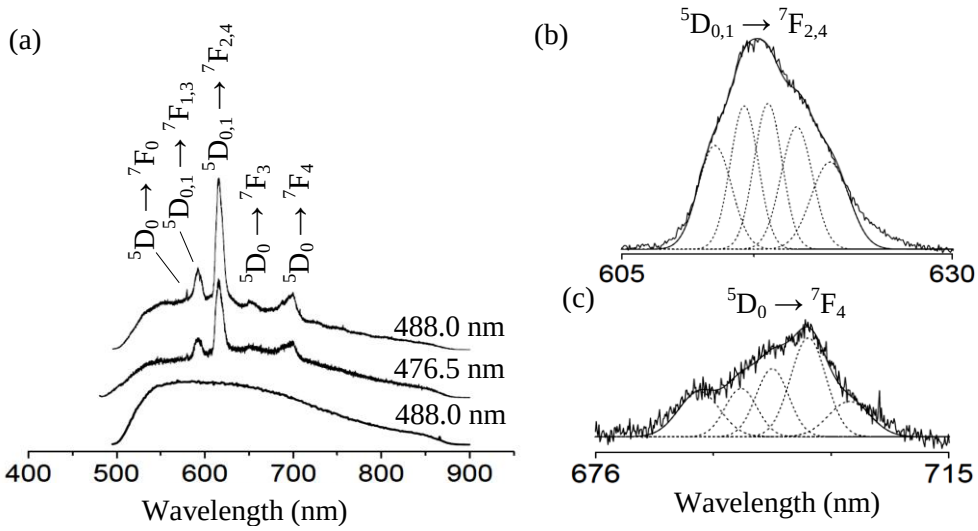

Figure 3. (a) Room temperature photoluminescence spectra of ZnO:Eu^{3+} and the undoped ZnO pellets. (b) and (c) Gaussian peak fitted emission bands.

Table 3. Crystal-field energy levels of the Eu^{3+} ion in ZnO in cm^{-1} (± 2 cm^{-1}).

Multiplet	$^7F_0$ (1)	$^7F_1$ (2)	$^7F_2$ (3)	$^7F_3$ (5)	$^7F_4$ (6)	$^5D_0$ (1)	$^5D_1$ (2)
Levels	0	373	919	1 849	2 568	17 259	18 847
			1 025	1 904	2 734		
			1 088	1 964	2 812		
				2 034	2 885		
				2 091	2 967		
					3 058		

emission for the same excitation conditions. The 457.9 nm excitation proved to be inefficient for populating the emitting multiplets while the 488.0 nm wavelength was the most suitable excitation line.

4. Conclusions

The XRD results showed no changes in the ZnO phase with the introduction of Tb^{3+} or Eu^{3+} ions. Room temperature Tb^{3+} and Eu^{3+} transitions in the visible region of the electromagnetic spectrum were observed in ZnO powders with excitation from the 457.9 nm, 476.5 nm and 488.0 nm argon laser lines. A total of 29 crystal-field energy levels for Tb^{3+} and 18 for Eu^{3+} were determined. The ZnO:Tb^{3+} and ZnO:Eu^{3+} emission transitions and energy level schemes are of significance for solid-state laser development and for optoelectronic device applications such as green and red light emitting diodes.

Acknowledgements

Financial support from the DST-NRF Centre of Excellence in Strong Materials (CoE-SM) and the University of the Witwatersrand, Johannesburg is gratefully acknowledged. We are also grateful to J. Augustine, C. Sandrock, V. Govender, L. Mafemba and G. Peters of the School of Physics, University of the Witwatersrand for their technical support.

References

[1] Kumar V, Som S, Kumar V, Kumar V, Ntwaeaborwa O M, Coetsee E and Swart H C 2014 *Chem. Eng. J.* **255** 541-552

[2] Podhorodecki A, Nyk M, Misiewicz J, and Strek W 2007 *J. Lumin.* **126** 219-224

[3] Ziani A, Davesnne C, Labbe C, Cardin J, Marie P, Frilay C, Boudin S and Portier X 2014 *Thin Solid Films* **553** 52-57

[4] Pal P P and Manam J 2013 *Mat. Sci. Eng. B* **178** 400-408

[5] Zhang J, Feng H, Hao W, and Wang T 2006 *Mat. Sci. Eng. A* **425** 346-348

[6] Yang L, Tang Y, Hu A, Chen X, Liang K and Zhang L 2008 *Phys. B* **403** 2230-2234

[7] Koao L F, Dejene F B, Kroon R E, and Swart H C 2014 *J. Lumin.* **147** 85-89

[8] Pereira A S, Peres M, Soares M J, Alves E, Neves A, Monteiro T and Trindade T 2006 *Nanotechnology* **17** 834-839

[9] Mote V D, Purushotham Y and Dole B N 2012 *J. Theoretical and Appl. Phys.* **6** 1-8

[10] Hufner S 1978 *Optical spectra of transparent rare earth compounds*. (New York: Academic Press) pp 1-13

[11] Koster G, Dimmock J O, Wheeler R G, and Statz H 1963 *Properties of the thirty-two point groups*. (Cambridge: M.I.T press) pp 55-57